# Surface-induced symmetry reduction in molecular switching: Asymmetric cis-trans switching of CH3S-Au-SCH3 on Au(111)

Guo, Quanmin

*DOI:*
10.1039/c6nr06864b



*Document Version*
Peer reviewed version

*Citation for published version (Harvard):*
Guo, Q 2016, 'Surface-induced symmetry reduction in molecular switching: Asymmetric cis-trans switching of CH3S-Au-SCH3 on Au(111)', *Nanoscale*. https://doi.org/10.1039/c6nr06864b

# Surface-Induced Symmetry Reduction in Molecular Switching: Asymmetric *cis-trans* Switching of $CH_3S$-Au-$SCH_3$ on Au(111)

**Jianzhi Gao[1], Lin Tang[2], Scott Holmes[3], Fangsen Li[4], Richard E Palmer[3], Quanmin Guo*[3]**

[1]*School of Physics and Information Technology, Shaanxi Normal University, Xi'an 710119, China.*

[2]*Department of Physics, Tsinghua University, Beijing, 100084, China.*

[3]*Nanoscale Physics Research Laboratory, School of Physics and Astronomy, University of Birmingham, Edgbaston, Birmingham, B15 2TT, United Kingdom.*

[4]*Vacuum Interconnected Nanotech Workstation, Suzhou Institute of Nano-Tech and Nano-Bionics, Chinese Academy of Sciences, Suzhou Industrial Park, Suzhou, 215123, China.*

**ABSTRACT**

*Cis-trans* isomerization of $CH_3S$-Au-$SCH_3$ driven by the tip of the scanning tunneling microscope is investigated at 77 K. $CH_3S$-Au-$SCH_3$ anchored on the Au(111) surface with the S-Au-S axis parallel to the substrate functions as a molecular switch due to the flipping of the $CH_3$ groups. The bonding between $CH_3S$-Au-$SCH_3$ and Au(111) leads to asymmetric isomerization where one of the two methyl groups flips much more effectively than the other, despite the symmetry of $CH_3S$-Au-$SCH_3$. Our findings suggest the possibility of constructing similar molecular switches that can be operated at room temperature and a potential route for fine-tuning of molecular switches in future nanoscale electro-mechanical devices.

KEYWORDS: *self-assembly; molecular switch; scanning tunneling microscopy; cis-trans isomerization; alkanethiol; gold.*

The mechanical movement within single molecules can be exploited to create molecular motors[1,2] and molecular switches[3,4]. Both motors and switches are essential components for the operation of a nano-mechanical system. Recent investigations performed on solid surfaces provide direct visualization of molecular switching[5-8]. A well-known example of molecular switches is azobenzene which undergoes *cis-trans* isomerisation under the influence of light[9,10]. A number of azobenzene derivatives have also been shown to be switchable when placed on a solid surface[7,11]. When molecules such as azobenzene are placed on a solid substrate, their switching behaviour becomes modified due to the interaction between the molecule and the substrate as well as that between neighbouring molecules[12,13]. This may result in significant suppression of switching[13] in comparison to that occurring in solution or in the gas phase. It is possible to choose an inert substrate and hence minimize molecule-substrate interaction[3]. However, the influence of the substrate can purposefully be used to control molecular switching or initiate new switching pathways[7]. Here we report the *cis-trans* isomerization of $CH_3S$-Au-$SCH_3$ on Au(111) and demonstrate that the molecule-substrate bonding can give rise to asymmetric switching where one of the two methyl groups is more switchable than the other.

$CH_3S$-Au-$SCH_3$, or Au-dimethylthiolate (ADM), is synthesized on the Au(111) substrate by exposing a (111)-oriented gold single crystal to dimethyldisulfide ($CH_3$-S-S-$CH_3$) vapour inside a vacuum chamber at room temperature according to the following scheme[14-16].

$$CH_3S\text{-}SCH_3 + Au = CH_3S\text{-}Au\text{-}SCH_3$$

The above scheme describes the overall reaction process. It is not yet clear if the dissociation of the disulfide is mediated by a Au adatom or Au atom is incorporated after the breaking of S-S bond. An earlier study with a similar molecule, $CH_3$-S-S-$(CH_2)_2CH_3$, suggests that pre-dissociation into $CH_3$-S- and $CH_3$-$(CH_2)_2$S- takes place before the incorporation of the Au atom[17]. STM studies[14,18,19,20] show that the Au atom of the ADM is bridge-bonded to substrate Au atoms while S sits above a Au atom in the Au(111) substrate. Therefore, ADM is anchored on the surface via three-point contact with the S-Au-S axis parallel to the substrate. The two $CH_3$ groups can flip leading to either *cis* or *trans* isomers of ADM[18,19]. An activation barrier of ~11 kcal/mol was reported based on calculations using the nudged elastic band method[19]. This suggests that thermally induced switching can take place at T~ 180 K[19]. The activation energy is expected to depend on both the chain length of SR and the strength of interaction between neighboring RS-Au-SR units. $CH_3S$-Au-$SCH_3$ on Au(111) behaves as an adsorbed molecule[14,18], although it does not exist in any form of a free molecule such as azobenzene. However, using electrospray ionization, Au-$(SCH_3)_2^-$ anions

have been successfully produced in the gas phase in an ion trap indicating the possible existence of neutral Au-$(SCH_3)_2$ species[21]. The electronic properties of neutral Au-$(SCH_3)_2$ has been studied theoretically using relativistic DFT methods[21]. If neutral Au-$(SCH_3)_2$ does exist like a single molecule, one wonders what would happen if these molecules are allowed to collide with each other? Perhaps they would spontaneously transform into thiolate-protected Au nanoclusters.

ADM forms a number of coverage dependent structural phases on Au(111)[14,16]. Here we concentrate on the striped phase at ~0.11 monolayer (ML) coverage. One monolayer is defined as one ADM per surface Au atom. The STM image obtained with –0.6 V sample bias and 1 nA tunnel current, Fig. 1(a), shows that the majority of the ADMs are found within regular rows parallel to one of the $<11\bar{2}>$ directions. As reported before, each ADM can be observed as a group of three bright protrusions: one from Au and two from the methyl groups[18,19]. Within the rows, ADMs are almost exclusively *trans* isomers. The two methyl groups from each *trans* ADM is at a distance ~ 0.7 nm. Along the $[11\bar{2}]$ direction, ADMs are regularly spaced at $\sqrt{3}a$ (0.5 nm) where $a$ is the nearest neighbour distance of Au atoms on the surface.

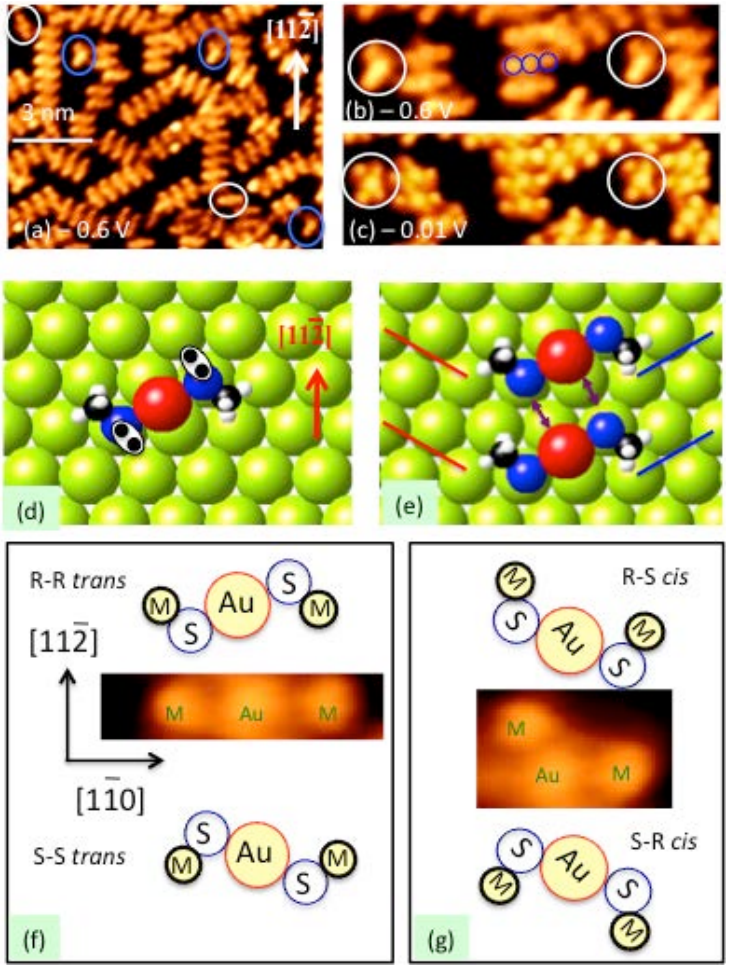


**Figure 1**. (a) STM image acquired with tunnel current of 1 nA and sample bias voltage of –0.6 V. White ovals mark isolated *trans* isomers of ADM; blue ovals mark isolated *cis* isomers. The ADM rows consist of all *trans* isomers. (b) and (c) STM images from the same area, acquired with different sample bias of –0.6 V and –0.01 V, respectively. (d) Ball model showing the bonding geometry of the ADM on Au(111). The red sphere represents the Au atom linking up two S atoms and the pair of black dots inside the oval represents the lone pair of electrons. (e) Formation of ADM rows via Au-S interaction. Blue and red bars indicate the two possible directions of the S-Au-S axis. (f) Schematics of the R-R *trans* and the S-S *trans* together with a representative STM image where "M" stands for the methyl group. (g) Schematics of the R-S *cis* and the S-R *cis* isomers and the corresponding STM image.

A small number of ADMs, those highlighted by the blue and white ovals in Fig. 1a for example, do not belong to any rows. These isolated ADMs are either *cis* (marked by blue ovals in the figure) or *trans* (white ovals) isomers. No *cis-trans* switching is observed with –0.6 V bias voltage, hence a *cis/trans* isomer remains as a *cis/trans* isomer under repeated scans. By keeping the tunnel current at 1 nA, reducing the bias voltage to less than 0.1 V leads to *cis-trans/trans-cis* switching. Figs. 1b and c show STM images from the same area but with different bias voltages. Two *cis* ADM isomers are marked by white circles in Fig. 1b, with each seen as a group of three spots. See Fig. 1g for a high-resolution image of a *cis* ADM. These two isolated *cis* ADMs look rather different under –0.01 V, Fig. 1c. Instead of three protrusions per ADM as seen in Fig. 1b, there are now five protrusions per ADM. This gives each ADM an outline shape of a "×". The appearance of two extra protrusions per

ADM under –0.01 V bias can be explained by *cis-trans* isomerization during the STM scan, resulting in a single ADM being imaged in both *cis* and *trans* configurations. The *cis-trans* isomerization involves the flipping of the methyl groups without any displacement of S or Au. Hence, the protrusion due to the Au atom remains unaffected by isomerization. Bias voltage induced changes to ADMs within the regular rows are also observed and will be discussed later.

Before going into detailed discussion of the *cis-trans* switching phenomenon, we will briefly review the general features regarding the bonding of ADM on Au(111). Fig. 1d shows how the ADM is attached to the Au(111) substrate[18] based on the current understanding: the S atom (blue sphere) sits almost directly above a Au atom in the substrate with the Au adatom (red sphere) occupying the bridge site. The two dots inside the oval shape above the S atom represent the lone electron pair on S. The S atom is a chiral centre[19] and Fig. 1d represents an R-R *trans* isomer based on the following order: $CH_3$, lone pair of electrons, Au atom beneath S, Au adatom (red sphere). Fig. 1e shows how two neighbouring R-R *trans* ADMs are held together by an electrostatic force between the positively charged Au and the negatively charged S. This kind of nearest neighbour interaction is responsible for the formation of ADM rows. A *trans* ADM on Au(111) can be either an R-R *trans* or an S-S *trans* as illustrated in Fig. 1f. The blue bars in Fig. 1e indicate the orientation of the S-Au-S axis for R-R *trans* isomers and the red bars for that of S-S *trans* isomers. For both R-R *trans* and S-S *trans*, the ADM appears as three protrusions aligned approximately along the $[1\bar{1}0]$ direction when imaged with the STM. For the *cis* ADM, it can take either the R-S *cis* or the S-R *cis* configuration as shown in Fig. 1g where the corresponding STM image of a *cis* ADM is also shown. The STM image here is to show the positional relationship between the three spots with no intension of showing the accurate orientation of the ADM.

Using the bonding scheme shown in Fig. 1d, we can now explain how an ADM can show up as a group of five protrusions in STM. *Cis-trans* isomerization under the STM can be induced by several stimuli including inelastic electron tunnelling[22]. By acquiring images with different bias voltages from –1 V to 1 V with the tunnel current fixed, we found that switching is independent of the bias polarity, but becomes more effective as the bias gets lower corresponding to smaller tip-molecule distances. From experiments with Au-diethylthiolate, we know that thermally–induced *cis-trans* isomerization does not take place even at room temperature[23]. This implies an activation barrier higher than 25 meV. Thus, 10 mV bias voltage is too low for electron-induced switching. The observed switching of ADMs can be understood by considering the force coming from the STM tip. There is always a van der Waals force and an electric field induced dipolar force, both are attractive and become

stronger as the tip-molecule distance in reduced. In Fig. 2, we use an R-R *trans* ADM as an example to demonstrate how an attractive interaction between the STM tip and the $CH_3$ group can lead to *cis-trans* switching. Assume the fast scan direction is the horizontal direction, as the scan line moves up, there will be a point at which the $CH_3$ group on the left flips down changing the ADM from R-R *trans* to S-R *cis*, Fig. 2b. As the tip moves further up, switching from S-R *cis* back to R-R *trans*, Fig. 2c, and then from R-R *trans* to R-S *cis*, Fig. 2d, can take place sequentially. During the whole series of switching illustrated in Figs. 2a-d, each $CH_3$ is imaged at two different locations and this is equivalent to a single complex like that shown in Fig. 2e being imaged once. Therefore, a single ADM appears in the STM image with five protrusions, Fig. 2f. The switching sequence illustrated in Fig. 2 depends strongly on tip-molecule interaction. This type of switching is different from the standard process in which a molecule changes from one stable state to another with a more permanent effect. The tip-induced switching discussed in this paper represents a dynamical switching behaviour. The fact that an alkyl chain can be imaged "simultaneously" at two different locations is not uncommon. Similar phenomenon is frequently observed whenever an atom or a molecule moves underneath the STM tip. Sometimes, one half of a single atom can be seen at one location and the other half of the same atom seen at a different location.

Although it is not the main object of the present research, switching probability as a function of tip-surface distance has nevertheless been investigated. This is performed by keeping the tunnel current constant and reducing the bias voltage step-by-step. Once the bias voltage is below 50 mV, the switching takes place with 100% probability. Above 0.5 V, the probability drops to zero. Similar to common procedures in atom manipulation, the condition of the tip is very important and parameters that are effective in switching the molecules depend on the condition of the tip. The force which manipulates the atom/molecule must be sufficiently localised to be effective.

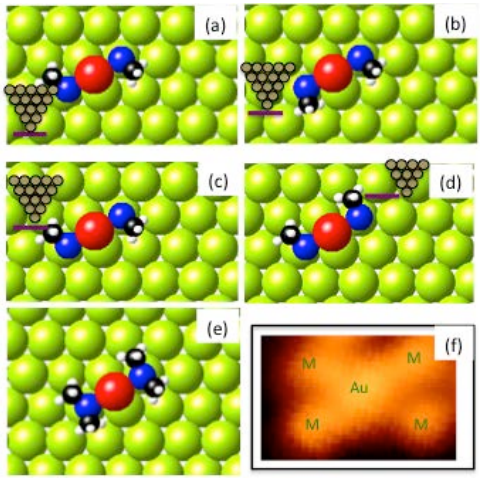


**Figure 2**. (a)-(d) Ball models showing the possible switching steps driven by an attractive force between the STM tip and the $CH_3$ group. The ADM starts as R-R *trans* in (a) and changes to S-R *cis* in (b), R-R *trans* in (c) and R-S *cis* in (d). The switching between the three isomers shown in (a) to (d) is equivalent to the presence of a single, fictitious, complex shown in (e) in terms of the signal detected by the STM. (f) Experimentally observed image of a single ADM obtained with 0.01 V sample bias. "M" stands for the methyl group.

We now turn our attention to the regular ADM row. The ADM row along the $[11\bar{2}]$ direction can be assembled by R-R *trans* ADMs as shown in Fig. 3a, or by S-S *trans* ADMs shown in Fig. 3b.

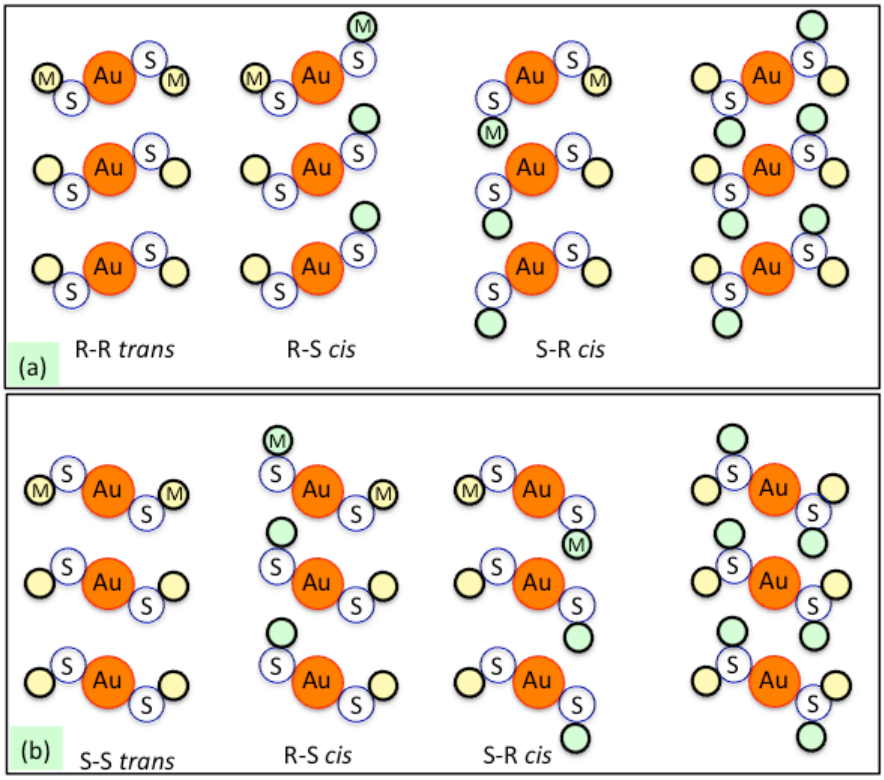


**Figure 3**. (a) The first column from the left shows a ball model for an R-R *trans* ADM row. The second column shows an R-S *cis* ADM row. The third column shows an S-R *cis* ADM row. The forth column indicates the experimentally observable structure due to *cis-trans* isomerization. Green circles represent $CH_3$ groups flipped from their initial positions in the R-R *trans* state. (b) Ball models for ADM rows originated from an S-S *trans* ADM row.

The first column from the left in Fig. 3a shows an R-R *trans* ADM row. Flipping the right hand $CH_3$ upwards changes the R-R *trans* ADM row to an R-S *cis* row shown in the second column. Similarly, an S-R *cis* row can be created by flipping the left hand $CH_3$ group downward. The last column is a superposition of the R-R *trans*, R-S *cis* and the S-R *cis* configurations. If all the *trans-cis/cis-trans* isomerization processes suggested in Fig. 3a take place under the influence of the STM tip, then five spots will be registered for each ADM. Fig. 3b shows similar isomerization processes for an initial S-S *trans* ADM row. Comparing Fig. 3a with 3b, one can see that starting from the R-R *trans* row, the $CH_3$ group on the left can flip downwards but not upward, while the $CH_3$ group on the right can only flip upward. The opposite is true for the S-S *trans* row, and hence we can use this different flipping behaviour to identify if a *trans* ADM row is an R-R or an S-S type. According to the ball model in Fig. 2, for an R-R *trans* ADM, it is equally possible for it to switch into an R-S *cis* or an S-R *cis*. This is because the $CH_3$ group at the left hand side is in a nearly identical chemical environment as the one on the right hand side. The observation of a "×"-shaped pattern for an isolated ADM, Fig. 2f, supports this view. However, when ADMs are assembled into rows, the ability of the two $CH_3$ arms to switch becomes distinctly different as discussed in the following.

Figure 4a shows an STM image of two ADM rows. The image is acquired using –0.01 V sample bias, so isomerization steps as described in Fig. 3 make each ADM appearing as five protrusions. However, one of the five protrusions for each ADM appears so faint that the ADM looks like having four protrusions. When imaging with –1 V sample bias, the four-ADMs in the upper row are found to take the S-S *trans* configuration while those in the lower row take the R-R *trans* configuration. For the lower five-ADM row, there is a characteristic protrusion, pointed by a solid yellow arrow, which is generated by the upward flipping of the right hand $CH_3$ group of the top most ADM. The flipping direction is indicated by a curved white arrow. In fact, such flipping of the right hand $CH_3$ group associated with the R-R *trans* to R-S *cis* isomerization is observed for all the five ADMs in the row. Moving to the bottom end of this ADM row, the ball model predicts a protrusion due to the downward flipping of the left hand $CH_3$ of the lowest placed ADM. The dotted yellow arrow points to the location where such a protrusion is expected. Although there is some signal intensity at the predicted position, the intensity is very low. This suggests that the downward flipping of the left hand $CH_3$ associated with the R-R *trans* to S-R *cis* transition is hindered. Thus, the R-S *cis* isomer occurs more frequently than the S-R *cis* isomer. The ball model beside the STM image illustrates the intensities of the observed protrusions. The dark green circles correspond to the higher intensity spots due to the upward flipping of the right hand side $CH_3$. The light green

circles correspond to the lower intensity spots from the downward flipping of the $CH_3$ at the left hand side.

For the S-S ADM row, the row consisting of four ADM units, the upward flipping of the $CH_3$ at the left hand side of the ADM is more effective making the R-S *cis* isomer the dominant *cis* isomer. Fig. 4b displays height profiles measured across lines PQ and MN in 4a. For the profile along PQ, the first peak (higher peak) corresponds to an up-flipped $CH_3$ and the second to a down-flipped $CH_3$. For the profile along MN, the first peak (lower peak) comes from down-flipped $CH_3$, and the second peak from up-flipped $CH_3$. Therefore, there appears to be a systematic difference in the effectiveness of $CH_3$ flipping. For a row of *trans* ADMs, no matter the starting ADMs are R-R *trans* or S-S *trans*, switching to the R-S *cis* configuration is always more effective than switching to the S-R *cis* configuration. The S-S row and the R-R row in Fig. 4a are oriented in the same direction and scanned under the same condition. The different switching behaviour of the two rows allows us to exclude the possibility that the observed phenomenon being caused by an asymmetric STM tip.

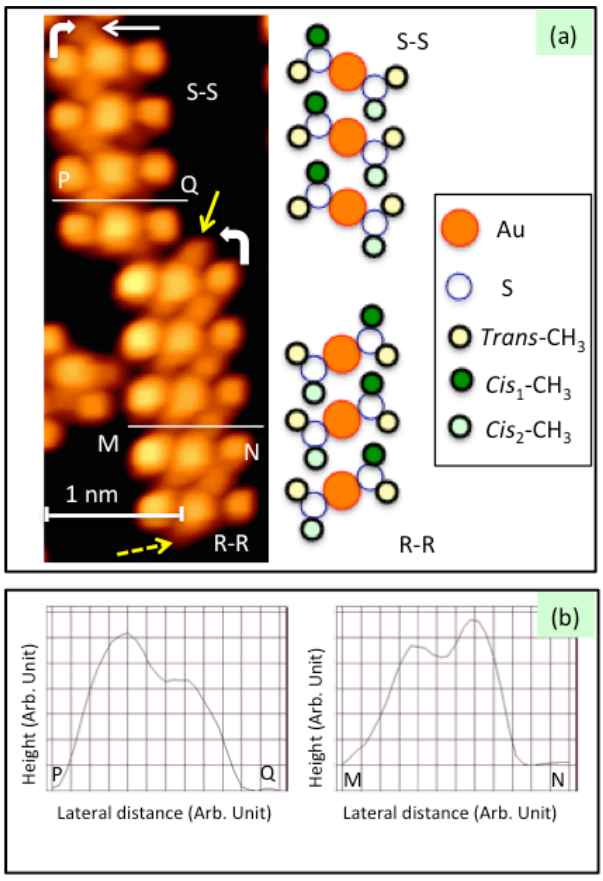


**Figure 4**. (a) S-S and R-R *trans* ADM rows. The solid yellow arrow points at the protrusion due to the upward flipping of the $CH_3$ group at the right hand side of the upper most ADM within the R-R row. The straight solid white arrow points at the protrusion due to the downward flipping of the $CH_3$ group at the left hand side of the

upper most ADM within the S-S row. The dotted yellow arrow points at the location of an expected protrusion. Ball models alongside the STM image illustrate the orientations of the *trans* R-R and S-S rows and the associated *cis* isomers. $Cis_1$ and $cis_2$ represent the protrusions coming from the dominant and the hindered *trans-cis* transitions, respectively. (b) Height profiles across lines PQ and MN in (a).

Data presented in Fig. 4 show that for ADM rows, the $CH_3$ group at one end of the ADM is more switchable than the one at the opposite end. The symmetry of $CH_3S$-Au-$SCH_3$ itself does not suggest such different switching behaviors for the two methyl groups. However, the interaction of $CH_3S$-Au-$SCH_3$ with Au(111) may change the symmetry. So far, the Au adatom of the ADM has been proposed to occupy the bridging position between two substrate Au atoms and the two S atoms are in identical adsorption site. The asymmetric switching phenomenon, however, indicates that the two S atoms may bond differently to the substrate. This could be achieved by shifting $CH_3S$-Au-$SCH_3$ sideways so that the Au adatom skews toward the nearest fcc site as shown in Figure 5. This sideway shift would make the two S atoms occupying slightly non-identical sites: one moving closer to the proper atop site and the other moving further away from the atop site. The non-identical bonding of the two S atoms would naturally lead to asymmetric switching of the methyl groups. Following the ball model in Fig. 1e, one can see that if the shift of an R-R *trans* ADM toward the nearest fcc site is directed to the right, then the shift for an S-S *trans* ADM must be directed to the left. Therefore, for the two ADM rows shown in Fig. 4a, the methyl groups on the left hand side of the S-S row are in the same environment as the methyl groups on the right hand side of the R-R row. The proposed shift of ADM towards the nearest fcc site is probably stabilised by the formation of the rows since switching for isolated ADMs shown in Fig. 1c appears to be much more symmetric. The proposed offset scheme for the Au adatom is in excellent agreement with the experimental observations, although we do not have other independent experimental evidence confirming such a scheme at this stage.

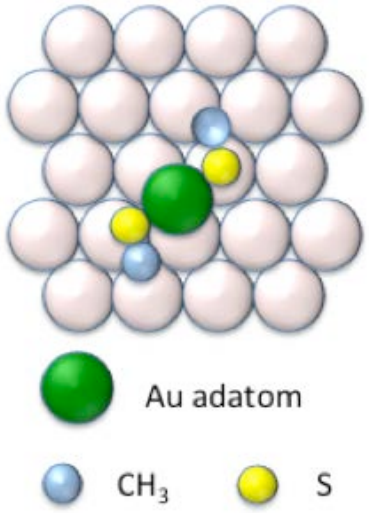


**Figure 5.** Adsorbed ADM with Au adatom shifted towards the nearest fcc hollow site, giving rise to non-identical bonding environment for the S atoms and hence asymmetric switching of the methyl groups.

Figure 6a shows an STM image consisting of a number ADM rows. There is a simple relationship between the row-row distance and the chirality of the ADMs. For two parallel rows, ADMs would take the same chirality in both rows if the following conditions are fulfilled. i) the two rows are separated by *na* along the $[1\bar{1}0]$ direction, where *n* is an integer, and ADMs in both rows have no positional offset along the $[11\bar{2}]$ direction. Rows AB, GH and IJ in Fig. 6a satisfy this condition and they are all R-R *trans* rows. ii) the two rows are separated by *(n+1/2)a* distance, and ADMs in one row are offset by $\sqrt{3}a/2$ relative to those in the other row along the $[11\bar{2}]$ direction. For instance, rows EF and GH meet this condition. Rows AB and CD are separated by *4a* distance, but row AB is R-R and row CD is S-S. This is because ADMs in row CD are shifted by $\sqrt{3}a/2$ relative to those in row AB. It is noted that the third ADM from the top in row GH is locked into an R-S *cis* configuration. The up-flipped $CH_3$ is the tallest $CH_3$ in the row. This tall $CH_3$ cannot flip down to the R-R *trans* position because of the close proximity of an ADM from an adjacent row to its right. In Fig. 6b and 6c, we show two more examples of steric hindrance on *cis-trans* isomerization. In Fig. 6b, the ADM marked with the white circle is locked into the R-S *cis* configuration. The ADM marked by a white circle in Fig. 6c is also locked into the R-S *cis* configuration. In each of these two cases, the locked *cis* isomer is prevented from flipping into the *trans* configuration due to the close proximity of a neighbouring ADM.

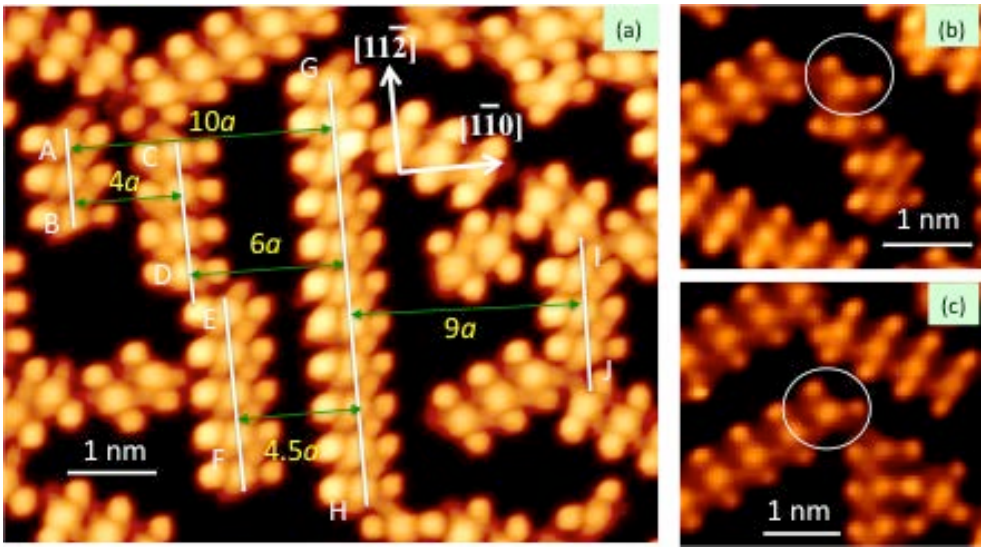


**Figure 6**. (a) STM image of ADM rows taken with –0.01 V sample bias and 1 nA tunnel current at 77 K. (b) and (c) STM images showing ADMs locked into the *cis* configuration as a result of hindrance from neighbouring ADMs.

We have observed similar *cis-trans* isomerization for Au-dipropyl-thiolate (ADP), $CH_3(CH_2)_2$S-Au-S$(CH_2)_2CH_3$, on Au(111). In this case, the propyl chain is longer than that of methyl by two carbon-carbon distances. Under most imaging conditions the propyl chains are observed as protrusions with the Au adatom invisible. Figure 7a shows a row of switching ADPs as observed with the STM at 176 K with –0.1 V sample bias and 0.2 nA tunnel current. The switching of ADP is observed at slightly longer tip-sample distances judged from the tunnel parameters used, suggesting a stronger tip-molecule interaction. The ADP row appears as two vertical rows of bright protrusions. The left row of protrusions in Fig. 7a are organized in a zig-zag fashion while the right row consists of vertically aligned protrusions. Moreover, for every protrusion in the right row there are two protrusions in the left row. This is due to the switching of the left propyl chain between the *trans* and *cis* configurations. The right chain remains stationary. Fig.7b shows a corresponding ball model illustrating the switching of the ADP. When the ADP row is imaged with greater tip-surface distance by using –1 V sample bias and 0.05 nA tunnel current, switching stops. Each ADP appears as a pair of bright protrusions as shown in Fig. 7c.

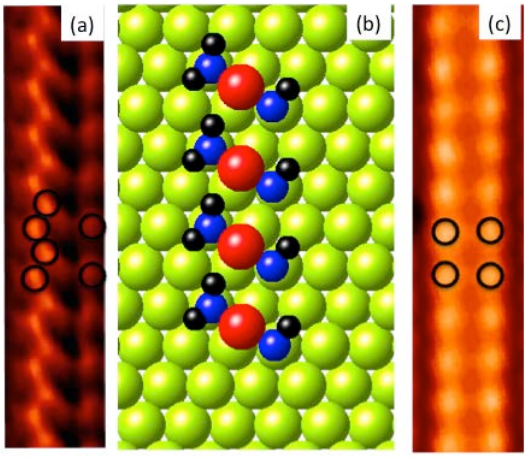


**Figure 7**. *cis-trans* isomerization of a Au-dipropyl-thiolate row. (a) STM image taken with –0.1 V sample bias and 0.2 nA tunnel current at 176 K. The black circles highlight the bright protrusions. There are two vertical rows of protrusions. For every protrusion in the right row, there are two protrusions in the left row due to the switching of the left arm of the ADP. (b) The structural model for the switching ADP. The propyl chain is represented by a single black sphere for clarity. Two black circles are shown to attach to the S atom on the left of the Au adatom to indicate the consequence of switching. (c) STM image obtained with –1 V sample bias and 0.05 nA tunnel current. Under this bias condition, the ADP takes the *trans* configuration and it does not switch, so every ADP shows up as two bright protrusions.

Under more extreme conditions, tip-molecule interaction can be strong enough to initiate symmetric switching. This happens with ADP when the tip-surface gap is further reduced by lowering the bias voltage. Figure 8 shows STM images and corresponding ball models for symmetric switching occurring with ADP. The images were acquired with –0.03 V sample bias and 0.4 nA tunnel current. With a sample voltage as low as –0.03 V, the Au atom as well as the propyl chains in the ADP appear as bright protrusions. By keeping the S-Au-S axis fixed and allowing the propyl arms at both ends to flip, we expect to observe five bright protrusions for each ADP: one from Au, four from the two propyl chains. In the STM image, we can group the bright protrusions according to the three possible configurations of each ADP: R-S *cis*, S-R *cis*, and R-R *trans*. In Fig. 8a, the green circle indicates the protrusion from the Au atom of the ADP, the blue and black circles are for the methyl groups of the ADP in the R-S *cis* configuration. Fig. 8b shows the expected protrusions from the S-R *cis* configuration. Circles in Fig. 8c show the positions of Au adatom and the propyl chains of ADP in the R-R *trans* configuration. The observed STM image is due to the combined contribution of ADP in all these three configurations.

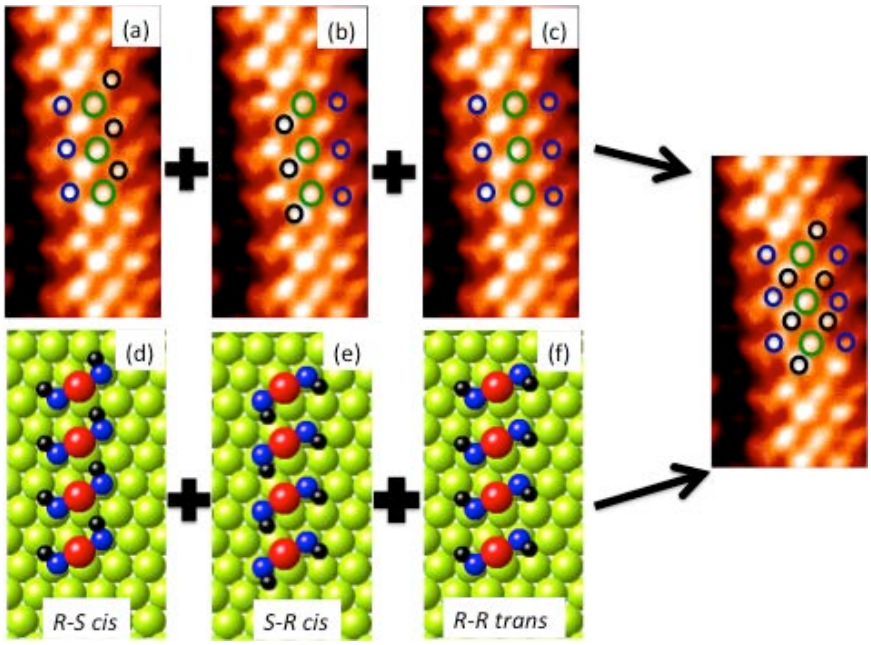


**Figure 8**. Symmetric switching of ADP. STM images in a, b and c are duplicates of the same image acquired using –0.03 V sample bias and 0.4 nA tunnel current at 115 K. Circles are overlaid onto the image to illustrate how the bright protrusions in the image are related to the configurations of ADP shown in the schematic diagrams in d, e, and f.

In summary, we have demonstrated asymmetric *cis-trans* isomerization of $CH_3S$-Au-$SCH_3$. Isomerization, proposed to arise from an attractive force between the STM tip and the $CH_3$ group, is most effective at small tip-substrate distances. Although the two $CH_3$ groups are energetically identical in $CH_3S$-Au-$SCH_3$, the bonding of ADM to the Au(111) substrate causes significant differences in the activity of the two $CH_3$ groups in *cis-trans* isomerization. In terms of making molecular switches, the isomerization of $CH_3S$-Au-$SCH_3$ on Au(111) gives a good example of fine tuning of the switching properties by making use of the bonding between the switchable molecule and the substrate.

## EXPERIMENTAL METHODS

We use the tip of the STM to induce *cis-trans* isomerization of ADM at 77 K. Experiments were performed using an Omicron low temperature STM operating at 77 K in an ultra-high vacuum (UHV) chamber with a base pressure $<10^{-10}$ mbar. A (111) oriented single crystal gold sample was used and cleaned by Ar+ ion sputtering and thermal annealing to 1000 K. Dimethyldisulfide vapour was introduced into the UHV chamber via a leak valve. The Au single crystal was kept under $5 \times 10^{-8}$ mbar of the vapour at room temperature for 15 minutes. The sample was then thermally annealed to 350 K before it was transferred to the STM chamber for imaging at 77 K. Electrochemically etched tungsten tips were used for

imaging under constant current mode. Work with ADP was performed in a separate UHV chamber where imaging was conducted using an Omicron variable temperature STM. A (111) oriented Au thin film supported on a highly-oriented pyrolitic graphite (HOPG) substrate was used for experiments with ADP.

## REFERENCES


[1] H. L. Tierney, C. J. Murphy, A. D. Jewell, A. E. Baber, E. V. Iski, Y. Khodaverdian, A. F. McGuire, N. Klebanov, and E. C. H. Sykes. *Nature Nanotechnol*. 2011, **6**, 625-629.

[2] U. G. E. Perera, F. Ample, H. Kersell, Y. Zhang, G. Vives, J. Echeverria, M. Grisolia, G. Rapenne, C. Joachim, and S-W. Hla. *Nature Nanotechnol*. 2013, **8**, 46-51.

[3] K. T. S. Kumar, T. Kamei, T. Fukaminato, N. Tamaoki. ACS *Nano,* 2014, **8**, 4157-4165.

[4] T. Leoni, O. Guillermet, H. Walch, V. Langlais, A. Scheuermann, J. Bonvoisin, and S. Gauthier. *Phys. Rev. Lett.* 2011, **106**, 216103.

[5] K. Kim, Y. H. Chang, S. H. Lee, Y. H. Kim, and S. J. Kahng. *ACS Nano,* 2013, **7**, 9312-9317.

[6] T. G. Gopakumar, T. Davran-Candan, J. Bahrenburg, R. J. Maurer, F. Temps, K. Truter, and R. Berndt. *Angew. Chem. Int. Ed*. 2013, **52**, 11007-11010.

[7] C. Dri, M. V. Peters, J. Schwarz, S. Hecht, and L. Grill, L. *Nature Nanotechnol*. 2008, **3**, 649-653.

[8] S. Ditze, M. Stark, F. Buchner, A. Aichert, N. Jux, N. Luckas, A. Gorling, W. Hieringer, H-P. Steinruck, and H. Marbach. *J. Am. Chem. Soc.* 2014, **136**, 1609-1616.

[9] G. S. Hartley. *Nature* 1937, **140**, 281-281.

[10] S. Monti, G. Orlandi, and P. Palmieri, *Chem. Phys*. 1982, **71**, 87-89.

[11] H.W. Kim, J. Jung, M. Han, S. Lim, K. Tamada, M. Hara, M Kawai, Y. Kim, and Y. Kuk. *J. Am. Chem. Soc.* 2011, **133**, 9236-9238.

[12] E. McNellis, J. Meyer, A. D. Baghi and K. Reuter. *Phys. Rev. B* 2009, **80**, 035414.

[13] Ch. Lotze, Y. Luo, M. Corso, K. J. Franke, R. Haag and J. I. Pascual. *J. Phys. Condens. Matter*. 2012, **24**, 394016.

[14] L. Tang, F. S. Li, and Q. Guo, *J. Phys. Chem. C.* 2013, **117**, 21234-21244.

[15] P. Maksymovych, O. Voznyy, D. B. Dougherty, D. V. Sorescu, and J. T. Yates. *Prog. Surf. Sci*. 2010, **85**, 206-240.

[16] L. Tang, F. S. Li, and Q. Guo. *Surf. Sci.* 2012, **606,** L31- L35.

[17] J. Z. Gao, F. S. Li, and Q. Guo. *Langmuir* 2013, **29**, 11082-11086.

[18] P. Maksymovych, D. C. Sorescu, J. T. Yates. *Phys. Rev. Lett*. 2006, **97**, 1461031.

[19] O. Voznyy, J. J. Dubowski, J. T. Yates P. Maksymovych. *J. Am. Chem. Soc*. 2009, **131**, 12989-12993.

[20] Q. Guo, and F. S. Li. *Phys. Chem. Chem. Phys*. 2014, **16**, 19074-19090.

[21] C-G. ning, X-G. Xiong, Y-L. Wang, J. Li, and L-S Wang, *Phys. Chem. Chem. Phys*. **2012**, 14, 9323.

[22] B. C. Stipe, M. A. Rezaei, and W. Ho, *Science*, 1998, **280**, 1732.

[23] F. S. Li, L. Tang, O. Voznyy, J. Z. Gao, and Q. Guo. *J. Chem. Phys.* 2013, **138**, 194707.

TOC graphic